

Fast and Adaptive Bulk Loading of Multidimensional Points

Moin Hussain Moti
HKUST
Hong Kong
mhmoti@connect.ust.hk

Dimitris Papadias
HKUST
Hong Kong
dimitris@ust.hk

ABSTRACT

Existing methods for bulk loading disk-based multidimensional points involve multiple applications of external sorting. In this paper, we propose techniques that apply linear scan, and are therefore significantly faster. The resulting FMBI Index possesses several desirable properties, including almost full and square nodes with zero overlap, and has excellent query performance. As a second contribution, we develop an adaptive version AMBI, which utilizes the query workload to build a partial index only for parts of the data space that contain query results. Finally, we extend FMBI and AMBI to parallel bulk loading and query processing in distributed systems. An extensive experimental evaluation with real datasets confirms that FMBI and AMBI clearly outperform competitors in terms of combined index construction and query processing cost, sometimes by orders of magnitude.

1 INTRODUCTION

In several applications (e.g., spatial/multimedia databases, recommendation systems), records can be represented as points in a multidimensional space. The coordinates of these points may correspond to locations in the Euclidean space, or the values of attributes of interest (e.g., ratings by critics/users). Queries request all records that satisfy some predicate, e.g., points within a multidimensional range, or those closest (i.e., most similar) to an input record. In the absence of an index, query processing necessitates a sequential scan of the entire data file, which is expensive due to the sheer volume of data in most applications. Multidimensional indexes enhance efficiency by pruning the parts of the data space that may not contain results. They can reside in main memory or be disk-based. Multidimensional disk-based indexes are the most common, as often the corresponding applications involve large amounts of data. They usually follow a tree structure with a single root. Internal nodes, called *branches*, hold entries of their children, which can be either other branches, or *leaves*, at the bottom tree level. Each node has a spatial extent, often shaped as a d -dimensional hyper-rectangle, where d is the dimensionality, that covers all points within its subtree.

Ideally, a multidimensional index should exhibit several, sometimes conflicting, characteristics. (1) It should be fast to build and update. (2) It should be space efficient, packing nodes close to their maximum capacity because half empty nodes have a negative effect on queries with large output. (3) It should minimize the total node area per level. (4) It should have shapely (i.e., square-like) node extents, avoiding nodes that are elongated on some dimension. Such nodes are likely to be accessed by many queries, even though they may not contain results. (5) It should minimize overlapping nodes at the same level because all such nodes are visited by queries that intersect the overlapping area.

When the data are given in advance, various bulk loading methods generate disk-based indexes using *external sorting*, as opposed to a distinct insertion per record. These methods differ on the order of level creation (*top-down* methods generate the root node first, while *bottom-up* create the leaf level), and the resulting index type. Conventional bulk loading creates the entire index in a single step. On the other hand, *adaptive indexes* are built progressively as a response to query processing. Consequently, parts of the index that contribute query results, are more refined than the rest. Although there has been some recent work on adaptive bulk loading for multidimensional points, it is focused on main memory.

In the following, we propose a novel bulk loading method for disk-based multidimensional points, which relies on scanning, as opposed to external sorting, and is much faster than existing techniques. The resulting index, called FMBI (Fast Multidimensional Bulkloaded Index) is very efficient for query processing as it exhibits the above desirable characteristics, including almost full and square nodes with zero overlap. In addition, we extend the proposed techniques to derive an adaptive version called AMBI (Adaptive Multidimensional Bulkloaded Index) that is refined using the query workload, gradually transforming to the final index. AMBI has a huge advantage compared to non-adaptive competitors, when the queries cover a small part of the data space, in which case only a partial index is generated. Our contributions are:

- (1) Novel scan-based techniques for bulk loading disk resident multidimensional points.
- (2) FMBI, a multidimensional index that exhibits excellent query performance, while it is several times faster to build than its competitors.
- (3) An adaptive version AMBI that builds the index on-demand according to the query workload, and avoids unnecessary work for parts of the data space that do not contribute query results.
- (4) Parallel versions of FMBI and AMBI, suitable for distributed systems and spatial partitioning.
- (5) A comprehensive experimental evaluation with real datasets that compares FMBI and AMBI with a multitude of existing indexes under a unified framework.

The rest of the paper is organized as follows. Section 2 presents related work. Section 3 describes the proposed bulk loading algorithms and FMBI. Section 4 extends our work to adaptive indexing and AMBI. Section 5 discusses parallel bulk loading in distributed systems. Section 6 contains the experimental evaluation, and Section 7 concludes the paper.

2 RELATED WORK

This section contains background material on multidimensional bulk loading and related areas.

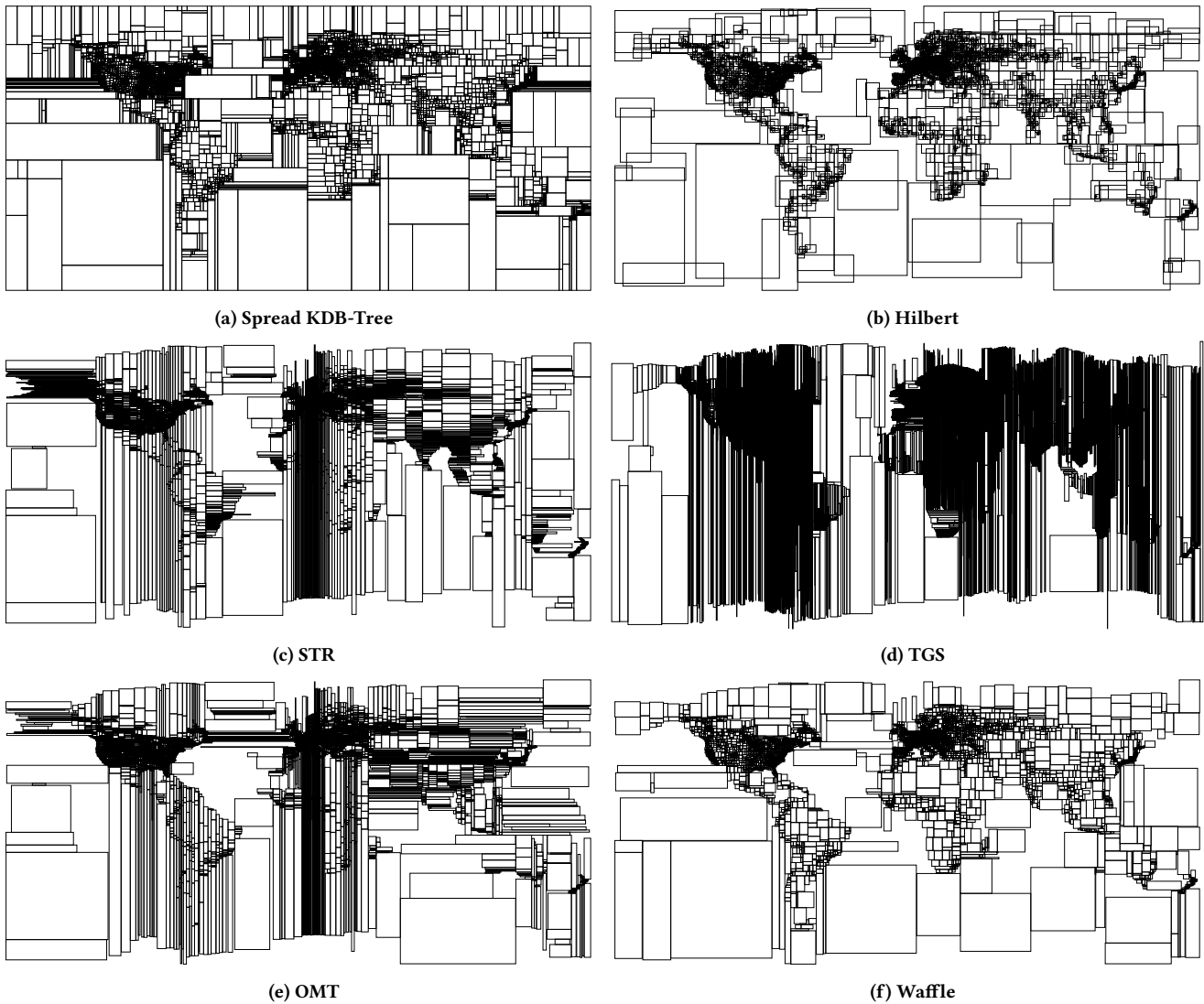


Figure 1: OSM leaf nodes created by bulk loading methods

2.1 Multidimensional Bulk Loading Methods

Multidimensional indexes are based on *space*, or *data* partitioning. In space partitioning schemes (e.g., KDB-Trees), the set of nodes at every level covers the entire data space. In data partitioning (e.g., R-trees), a node’s spatial extent is the minimum bounding box (MBBs) covering its entries, so that there may exist empty spaces not covered by any node. Various methods bulk load both index types starting from the root (top-down) or the leaf level (bottom-up).

KDB-Trees [33] are considered the most effective space partitioning index. They can be bulk loaded using a top-down process [24], which begins with a single node holding all the pages and covering the entire space. Partitioning is performed by sorting the pages on a selected dimension, and splitting on the median entry. If the resulting subspaces overflow, they are recursively split. KDB-Tree variants are differentiated on the choice of split dimension. *Cyclic*

KDB-Trees [33] alternate the split dimension, while *Spread* KDB-Trees [14] select the longest dimension, i.e., the one with the highest data-spread.

A number of methods bulk load R-trees bottom-up. In Hilbert Packing [19] the set of data points is first sorted on their Hilbert rank [13]. Then, groups of C_L consecutive sorted points, where C_L is the leaf node capacity, are packed into disk pages, which form the bottom level (i.e., leaf nodes). The same procedure is applied to the nodes of the next level, all the way to the root, using a corner or center of a node’s spatial extent to compute its Hilbert rank. Essentially this method generates an 1D order (based on the Hilbert rank) of multidimensional objects. Alternative techniques can be based on different space filling curves [1] [32], or simply on sorting on a single dimension [34]. Such methods achieve full disk pages, but may lead to overlapping nodes.

STR [22] is a bottom-up procedure based on sorting and tiling. Given a 2-dimensional dataset of N points, the number of pages required for the leaf level is $P = \lceil N/C_L \rceil$. The dataset is sorted on the x -axis, and the points are *tilled* to $\lceil \sqrt{P} \rceil$ vertical slices. Slices with more than C_L points are sorted and tiled on the y -axis. The slices that remain after all overflows have been resolved form the leaf level of the R-tree. The process is repeated recursively for the resulting nodes to create subsequent levels, until there is a single root. STR can be adapted to d -dimensional ($d > 2$) datasets by tiling $\lceil P^{\frac{1}{d}} \rceil$ slices for each dimension.

TGS [15] is a top-down bulk loading procedure for the R-Trees. The root (of a subtree) is created by repeatedly partitioning its P pages into two sets, until there are $\lfloor C_B \rfloor$ subsets, each containing $\lceil P/C_B \rceil$ pages, where C_B is the branch capacity. For each partition, TGS considers $O(C_B)$ splits in every dimension to identify the split that minimizes a given cost function (e.g. sum of the volumes of the MBBs). This process is recursively applied to the root’s child nodes to build the R-Tree. TGS is very expensive to build [3, 32, 40], and has fluctuating query performance [32].

OMT [21] is a top-down variant of STR that starts with a root containing the entire dataset. The height of a branch node n is computed as $h = \lceil \log_{C_B} P_n \rceil$, where C_B is the branch capacity, and P_n is the total number of pages contained in n . Since n is at height h , all its child nodes would contain $P_{\text{child}} = C_B^{h-1}$ number of pages, implying that n has $\lceil P_n/P_{\text{child}} \rceil$ child nodes. Similar to STR, the pages are sorted and tiled, so that each dimension has $\lfloor |n|^{\frac{1}{d}} \rfloor$ tiles. The tiles that contain a singular page become leaf nodes, and the tiles with multiple pages undergo the packing procedure recursively.

Waffle [24] uses a bottom-up bulk loading procedure that involves two steps. A first step creates the leaf level by recursively sorting and splitting the data points on the longest dimension, until each resulting subspace contains a single page. The split point corresponds to the entry that is nearest to the median and at the boundary of one of the pages, i.e. the entry ranked $C_L \times \lfloor \frac{\lceil N/C_L \rceil}{2} \rfloor$. To create the next level, a second step reuses splits created for the leaf level in the order of their creation. The splitting stops when no subspace exceeds C_B leaf nodes. This continues recursively until at most C_B nodes remain at the top, which form the child nodes of the root. Waffle, similar to STR and OMT, incurs zero overlap between nodes at the same level.

Figure 1 displays the leaf nodes of various bulk loaded indexes for 3 million points¹ of the OSM dataset [28] (1 billion points). The disk page size is set to 4KiB, yielding a maximum leaf node capacity of $C_L = 341$ points for all indexes. Table 1 illustrates the number of leaf nodes, and the total area and perimeter of leaf nodes for each method on the full dataset. KDB-Trees do not emphasize on space utilization and involve a high count of leaf nodes. R-tree packing schemes and Waffle achieve the minimum number of leaf nodes because they are fully packed. The total area of Hilbert-Tree leaf nodes exceeds the data space because of node overlaps. STR, TGS, and OMT have low total area, but high perimeter due to elongated nodes. In TGS, as suggested by its authors, we use the split that minimizes the sum of the area of the resulting partitions. Notably,

¹We only use 3 million points because the leaf nodes of the full dataset are too dense to visualize.

Index	Count	Perimeter	Area
KDB-Tree	4194304	0614769	064280
Hilbert	2932552	1983297	137157
STR	2932552	1470623	049308
TGS	2932552	100757580	046245
OMT	2932552	1235628	039789
Waffle	2932552	0436979	039389

Table 1: Total count, perimeter, and area of leaf nodes

the splits only minimize the area for the immediate partitions, and does not necessarily result in minimum area for the whole index. Moreover, this produces elongated nodes with the highest perimeter, consistent with the findings reported in [40]. Waffle creates the partitions with the best characteristics, but as shown in the experimental evaluation, it is expensive to build.

In recent years there is a large amount of work on *learned* indexes that replace internal nodes with machine learning models (e.g., artificial neural networks), or utilize machine learning to enhance the index capabilities. Several multidimensional learned indexes (e.g., Flood [25], Tsunami [8]) assume a known data distribution and query workload, or involve approximate querying (e.g., RSMI [31]). Moreover, they focus primarily on in-memory operations and lack in the spatial domain (e.g., not supporting k NN queries [25, 38]). Even disk-based learned indexes such as LISA [23], and PLATON [40] are very slow to build since they involve model training. For instance, PLATON uses Monte Carlo tree search to build models based on a given workload. While all the aforementioned conventional bulk loading methods require under an hour to bulk load the full OSM dataset, PLATON takes about 10 hours for 10% of the dataset. Since our aim is efficient index building, we do not consider learned multidimensional indexes as competitors of the proposed methods.

2.2 Other Related Work

Bulk loading generates a complete and fixed index, independently of the query workload. On the other hand, *adaptive indexes* are generated progressively as a response to query processing [20]. Consequently, parts of the index that participate in more queries, are more refined than the rest. Recently the concept of adaptive indexes has received attention in *database cracking* [17]. QUASII [30] is an adaptive KDB-Tree based index that applies cracking to one dimension per tree level. At the top level, QUASII cracks along the query’s extent on the first dimension generating a piece on that dimension. Then, at the next level it indexes the piece corresponding to the query’s extent on the second dimension, and so on. After the query is processed, the index is a wide tree of D levels, each associated with a single dimension. AKD (adaptive KD-tree) [26] is based on a similar idea, but it adds up to $2D$ new tree levels, one for each bound along each dimension. Unlike QUASII and AKD, which index one dimension per level, the AIR-tree [42] maintains all dimensions at each level. The index is a main memory R-tree, generated incrementally, by splitting nodes that intersect incoming queries. Nodes stop being cracked, when their entries fall below a threshold, in which case the index reaches its steady state. [18]

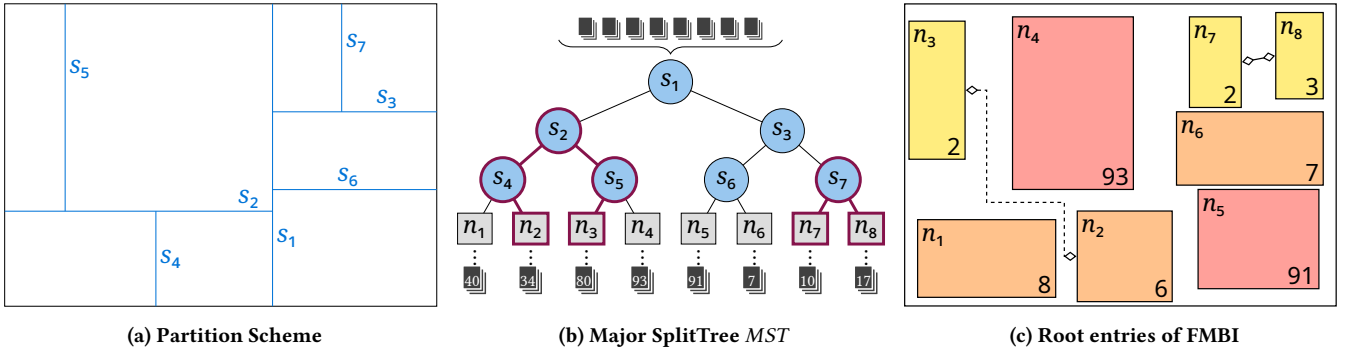


Figure 2: FMBI Example

contains an experimental evaluation of multidimensional adaptive indexes for main memory.

The term *adaptive indexing* has also been used in different contexts. In [35], it refers to indexes where the node size (i.e., number of disk pages per node) is based on the data and query characteristics (e.g., in parts of the data space where range queries have large extents, nodes may occupy multiple pages). Assuming that the query distribution is known in advance, [1] bulk loads an R-tree optimized for the query workload. In both [35] and [1] the index is full, as opposed to progressively refined.

Spatial partitioning is the process of dividing an entire space into multiple disjoint subspaces that are usually managed by different servers. Each server receives and processes queries about data within its own subspace. A number of systems ([9, 11, 12, 39, 41]) apply STR [22] based techniques to perform space partitioning. R*-Grove [37] samples the data points and partitions the space using the R*-Tree split algorithm [5]. SATO [36], also based on sampling, aims at minimizing the number of multidimensional objects crossing partitions. [29] studies the problem of parallel bulk loading for spatial data reside in distributed servers.

3 FULL BULK LOADING AND FMBI

This section describes techniques for bulk loading the full index, called FMBI (Fast Multidimensional Bulkloaded Index). FMBI utilizes concepts of both data and space partitioning. Specifically, similar to R-trees, the node extents are minimum bounding boxes (MBBs) that tightly cover the underlying entries. On the other hand, node splits occur on the median of the longest dimension, similar to Spread KDB-Trees. Bulk loading is top-down and involves five concrete steps.

Step 1: Initial Partitioning

We assume a main memory buffer of M pages, such that $M > C_B$ where C_B is the branch capacity. The bulk loading process starts by reading $\alpha \cdot C_B$ random pages of the dataset, where $\alpha = \lfloor M/C_B \rfloor$, and sorting their points in-memory, on the longest dimension. The last point of the $\lfloor (\alpha \cdot C_B)/2 \rfloor^{\text{th}}$ sorted page is the partition point, and its coordinate on the longest dimension, constitutes the split, which becomes the root of a *Major SplitTree*, referred to as MST . Based on the split point, the first $\lfloor (\alpha \cdot C_B)/2 \rfloor$ sorted pages form the

first subspace, while the rest form the second subspace². Next, we recursively partition these subspaces on their longest dimension, until each subspace contains α pages. For every new split point, a pointer is stored in its parent at MST . If the split dimension changes (between a split point and its parent), sorting on the new dimension is required, but it is always performed in main memory. Once completed, MST contains $C_B - 1$ splits that partition the space into C_B subspaces, each with α full pages.

Figure 2 shows an example assuming branch node capacity $C_B = 8$. The first split s_1 occurs on the (longest) x -dimension, while its children s_2 and s_3 are split on the y -axis. At the end of Step 1, there is a total of 7 split points and 8 subspaces. In addition, we maintain the MBBs of the subspaces, which will form into FMBI root entries during the subsequent steps.

Step 2: Distribution of Remaining Pages

This step distributes the points of the remaining pages (excluding the $\alpha \cdot C_B$ pages already scanned) into the subspaces of Step 1. Initially, each subspace is deemed to be *active*, and its α full pages are kept in main memory. At the first insertion in some subspace, we allocate it a new buffer page. A search on MST determines the subspace covering each data point p ; p is inserted in the corresponding buffer page, and the MBB of the subspace is adjusted if necessary. If the buffer reaches its limit when allocating a new page to an active subspace, we flush all its full pages to the disk, which renders it *inactive*. Each inactive subspace retains a single memory page, which is flushed when it fills. When all points have been exhausted, Step 2 terminates. Continuing the running example, the number of pages after Step 2 is shown below each subspace in Figure 2b.

Step 3: Refinement of Sparse Subspaces

The goal of this step is to create the FMBI subtree for each subspace that can fit in the available buffer, referred to as *sparse*. Active sparse subspaces are processed first because their pages are already in-memory. Algorithm 1 describes the recursive procedure, where the initial input is the list of pages of a subspace n , and the final output is the list of entries of the corresponding FMBI node. The procedure follows a post-order traversal of a *minor SplitTree* for n (mST_n), where at each mST_n node visit, it processes a list of pages,

²Using the above mechanism, all points of each sorted data page are assigned to the same subspace.

\mathcal{P} . If $|\mathcal{P}| = 1$, it returns a FMBI leaf node entry generated from that single page. Otherwise, it sorts the points of \mathcal{P} on the longest dimension, and partitions them into two halves, \mathcal{P}_1 and \mathcal{P}_2 , with $\lfloor |\mathcal{P}|/2 \rfloor$ and $\lceil |\mathcal{P}|/2 \rceil$ pages, respectively. The two halves undergo the same process recursively, returning two sets of entries ne_1 and ne_2 . If the sum of entries does not exceed C_B , the output is a concatenated list of ne_1 and ne_2 . Otherwise, Algorithm 1 returns two FMBI branch node entries nb_1 and nb_2 , generated from ne_1 and ne_2 .

Algorithm 1 Procedures for refining subspaces

```

1: procedure GENERATE_ENTRIES(Page[]  $\mathcal{P}$ )
2:   if  $|\mathcal{P}| = 1$  then
3:      $nl \leftarrow$  leaf node entry of  $\mathcal{P}$ 
4:     return [ $nl$ ]  $\triangleright$  List containing a single entry
5:   Sort points of  $\mathcal{P}$  on longest dimension
6:   Partition  $\mathcal{P}$  into  $\mathcal{P}_1$  and  $\mathcal{P}_2$ 
7:   NodeEntry[]  $ne_1 \leftarrow$  generate_entries( $\mathcal{P}_1$ )
8:   NodeEntry[]  $ne_2 \leftarrow$  generate_entries( $\mathcal{P}_2$ )
9:   if  $|ne_1| + |ne_2| \leq C_B$  then
10:     $ne \leftarrow$  Concatenated list of  $ne_1$  and  $ne_2$ 
11:    return  $ne$ 
12:   else
13:     $nb_1 \leftarrow$  branch node entry of  $ne_1$ 
14:     $nb_2 \leftarrow$  branch node entry of  $ne_2$ 
15:    return [ $nb_1, nb_2$ ]  $\triangleright$  List containing  $nb_1$  and  $nb_2$ 

```

Figure 3 illustrates the application of Algorithm 1 on n_3 containing 80 pages (see Figure 2b), and the corresponding minor SplitTree mST_3 . For each mST_3 node, the left cell shows the number of pages received as input, and the right cell the number of FMBI node entries returned. The post-order traversal starts from the root and first creates two FMBI leaf entries nl_{64}, nl_{65} that correspond to the two leftmost leaf nodes t_{64} and t_{65} of mST_3 . When Algorithm 1 backtracks to their parent t_{32} , since $|nl_{64}| + |nl_{65}| = 2 < 8$, it returns the concatenation of nl_{64} and nl_{65} to t_{16} , which in turn outputs five concatenated entries (nl_{64}, \dots, nl_{69}) to t_8 . At t_8 the total number of input entries (10), received from t_{16} and t_{17} , exceeds $C_B = 8$. This leads to the addition of two FMBI branch entries nb_{16} and nb_{17} , corresponding to mST_3 nodes t_{16} and t_{17} . The process continues all the way to the root of mST_3 , where two FMBI root entries are created for t_2 and t_3 . The grey cells indicate mST_3 nodes that generate FMBI entries. The bottom right corner of Figure 3 illustrates a simpler case for n_6 , whose subspace is divided into 7 FMBI leaf entries, each corresponding to a leaf node of mST_6 .

When an active subspace is finalized, its buffer pages and mST are released from main memory. After all active subspaces are processed, each inactive sparse subspace is reloaded and refined in the same way. Figure 2c indicates for each sparse subspace, its MBB and the number of root entries of their FMBI subtree after refinement. Subspaces n_4 and n_5 are *dense*, i.e., their size exceeds the available buffer, and will be processed at Step 5.

Step 4: Merging of Underflowed Branches

Branch nodes with no more than $C_B/2$ entries (e.g., n_3, n_7, n_8 in Figure 2c) are *underflowed*. To mitigate their negative effect on

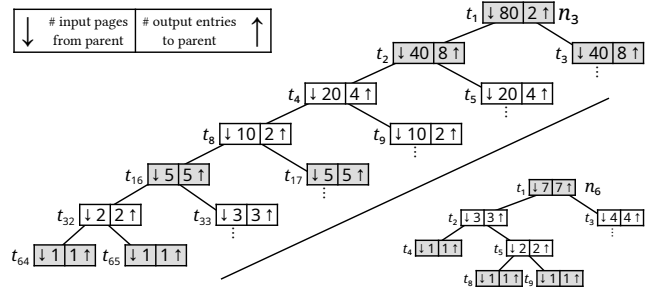


Figure 3: Minor SplitTrees of n_3 and n_6

Algorithm 2 Procedure for merging the branches

```

1: procedure MERGE_BRANCHES(Pointer  $ptr$ )
2:   if  $ptr$  points to a leaf of MST then
3:      $n \leftarrow$  MST node pointed by  $ptr$ 
4:     if  $n$  is processed then return  $n$ 
5:     else return  $\phi$   $\triangleright n$  is dense (not processed)
6:    $s \leftarrow$  split pointed by  $ptr$ 
7:    $n_l \leftarrow$  merge_branches(left pointer of  $s$ )
8:    $n_r \leftarrow$  merge_branches(right pointer of  $s$ )
9:   if  $n_l$  is  $\phi$  then return  $n_r$ 
10:  if  $n_r$  is  $\phi$  then return  $n_l$ 
11:  if total number of entries in  $n_l$  and  $n_r$  is within  $C_B$  then
12:    return merge( $n_l, n_r$ )
13:  else
14:    if  $n_l$  has fewer entries than  $n_r$  then return  $n_l$ 
15:    else return  $n_r$ 

```

query performance, we invoke a bottom-up strategy that merges them *conceptually*. Concretely, we perform a post-order traversal of the Major SplitTree, where for each underflowed branch n_u , we find the subspace n_v with the lowest common ancestor to n_u at the MST, such that the total number of their entries is within C_B . The aggregated contents of both nodes are stored on the same disk page, but the root of FMBI maintains two separate entries for n_u and n_v . This process does not introduce additional I/O during query processing since merged pages are only accessed if some of their nodes potentially contain query results.

Algorithm 2 describes the pseudocode for merging. The input is a pointer ptr , which initially points to the root of MST. A recursive call terminates when ptr points to a subspace. If the corresponding node n is processed (i.e., sparse), the call returns n as a candidate for merging. Otherwise, if n is dense, it returns ϕ . When ptr points to a split s , the recursive calls to its left and right subtrees return n_l and n_r . If one of n_l or n_r is ϕ , the other node is returned without attempting to merge (this also covers the case where both n_l and n_r are ϕ). If the total number of entries of n_l and n_r is within C_B , n_l and n_r are merged. Otherwise (no merge is possible) the algorithm returns the node with the fewer number of entries, as a potential candidate for merging upstream. After the algorithm terminates, there is at most one underflowed branch remaining and MST is deleted.

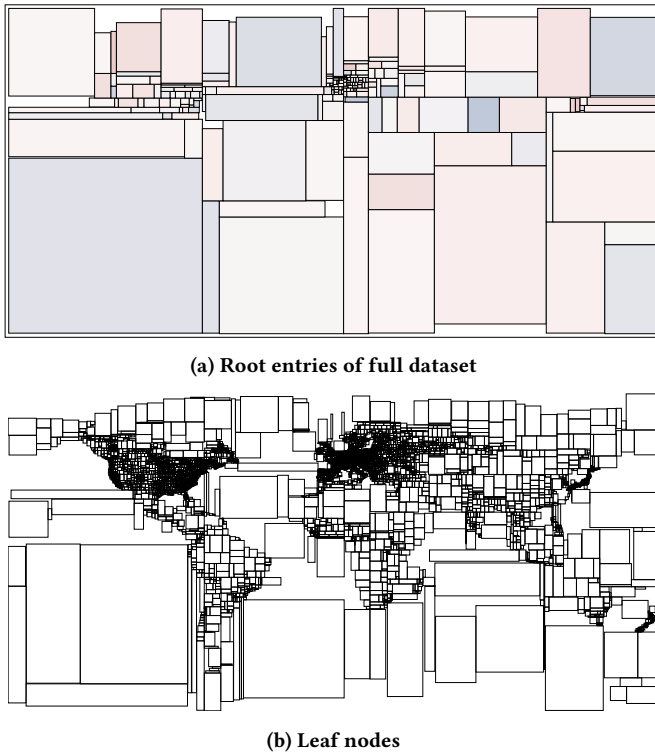


Figure 4: FMBI bulk loaded with OSM

In the example of Figure 2, the initial input of Algorithm 2 is the root s_1 of MST . The processing of s_4 returns n_2 since it has fewer entries (6) than its sibling n_1 (8). Similarly, s_5 returns n_3 , as n_4 is dense and unprocessed. After receiving n_2 and n_3 , s_2 merges them, and their entries (6 and 2, respectively) are stored in the same disk page. In the right subtree, n_7 and n_8 are merged at s_7 with a total of 5 entries in their shared disk page.

Step 5: Processing of Dense Subspaces

Since dense subspaces (e.g., n_4 , n_5) contain more data pages than the available buffer, they cannot be refined using Steps 3 and 4. Instead, each dense subspace n is treated as new dataset to be bulk loaded. Accordingly, we apply all steps to the data points of n and generate an index $FMBI_n$. The root of $FMBI_n$ becomes an entry in the root of FMBI.

Figure 4a shows the root entries of the final FMBI, after bulk loading OSM (the full dataset). The color of each subspace indicates the number of entries in its subtree, where red (grey) subspaces have more (fewer) points than average. Nevertheless, the variance is rather small, as the cardinality of the subspace with the maximum (minimum) number of entries is 1.06 (0.92) times that of the average, suggesting that FMBI is rather balanced. Figure 4b displays the leaf nodes of FMBI under the same settings as in Figure 1. When bulk loaded with the full OSM dataset, FMBI has 2932651 leaves, with total perimeter 432743, and area 39310. Comparing with Table 1, FMBI has marginally more leaves than the fully packed indexes, while exhibiting the lowest total area and perimeter.

4 ADAPTIVE BULK LOADING AND AMBI

Similar to the other multidimensional indexes, the proposed techniques apply top-down traversal for query processing. A query starts from the root, and recursively visits each node that may contain results. The search terminates at leaf nodes, where the corresponding pages are scanned and filtered to aggregate all qualifying points. Whereas conventional indexes, including FMBI, are built in advance (i.e., before the first query), in AMBI (Adaptive Multidimensional Bulkloaded Index) the index is built on-demand, when unprocessed nodes are encountered during query processing. We assume that the query type or distribution is not known in advance.

4.1 Query Based Index Refinement

In the absence of an index, each query necessitates a sequential scan of the data file. When the first query is received, AMBI initializes the root with Step 1, i.e., by loading $\alpha \cdot C_B$ pages in-memory and building the major SplitTree MST . Similar to FMBI, at Step 2 all subspaces of MST are initially *active*, and their pages are kept in-memory, while the rest of the dataset is distributed. However, instead of deactivating the subspace when the buffer reaches its limit, AMBI maintains a max-heap H of active subspaces based on their Euclidean distance from the query, and flushes the top of H . Consequently, subspaces that are *unqualified* (i.e., those not containing query results) are deactivated first, whereas those that are *qualified* are kept in main memory.

Eventually, even qualified subspaces may have to be deactivated, but more strategically. If a qualified subspace n contains $P_n < C_B$ pages, it is deactivated in the same way as an unqualified one. Otherwise, when $P_n \geq C_B$, AMBI generates its minor SplitTree mST_n using $\beta \cdot C_B$ pages, where $\beta = \lfloor P_n / C_B \rfloor$. All mST_n subspaces are added to H based on their distance from the query, so that they too become candidates for deactivation³. Any remaining pages of n are distributed to mST_n 's subspaces. This process may be repeated recursively until the buffer is freed.

Figure 5 shows the partitions of Figure 2 in the context of adaptive indexing for a window query q (red rectangle). Following Step 1, the space is partitioned into $C_B = 8$ subspaces n_1 to n_8 , which are inserted to H . As the buffer gets full during Step 2, subspaces are deactivated (highlighted in grey) in the reverse order of their distance from q . If the buffer fills when H only contains qualified subspaces n_3 and n_4 , n_4 is partitioned into $n_{4.1}$ to $n_{4.8}$ that replace n_4 in H . Some of those subspaces (shown in blue) are also subsequently deactivated. When distribution terminates the active subspaces are n_3 , $n_{4.1}$, $n_{4.2}$, $n_{4.3}$ and $n_{4.5}$.

All active subspaces, including unqualified $n_{4.3}$, $n_{4.5}$, are refined by Algorithm 1 as they do not incur additional I/O cost. On the other hand, AMBI does not refine any inactive subspace n_u , whether sparse or dense. Instead, n_u will be processed when it qualifies for some query in the future, using a minor SplitTree (if n_u is sparse) or a major SplitTree (if n_u is dense). Observe that an inactive subspace n_u , with $P_{n_u} < C_B$ pages will always generate P_{n_u} leaf entries when processed. Thus, we can safely merge an unrefined subspace with a processed one, provided that their total number of entries is

³The subspaces of mST_n are less likely to be useful and more likely to contain fewer than C_B pages, which makes them suitable for deactivation.

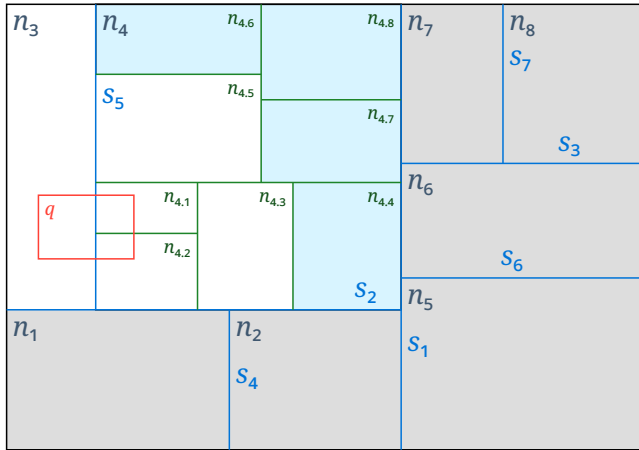


Figure 5: Adaptive subspace partitions

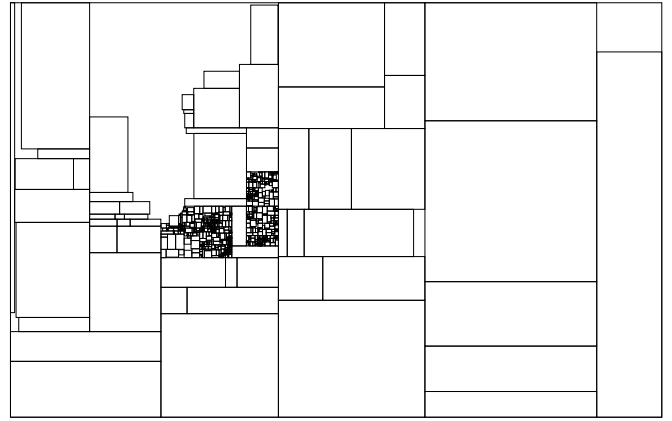
within C_B . This enables us to include all subspaces, irrespective of their constitution, in the merging process of Algorithm 2. Naturally, nested subspaces are merged first, so that finalized entries of useful subspaces can participate in the merging at the root of MST .

Figures 6a and 6b illustrate the partial index generated by AMBI after 10 and 100 window queries focused on Germany. Only nodes containing data points in or around Germany are fully refined into leaf nodes. The rest of MBBs correspond to higher level nodes that remain unprocessed. It is important to note that unlike other adaptive indexes (e.g., AIR [42]), where the final tree depends on the order of queries, the set of AMBI nodes is independent of the query order. If the queries cover the entire data space, AMBI becomes identical to FMBI as shown in Figure 6c.

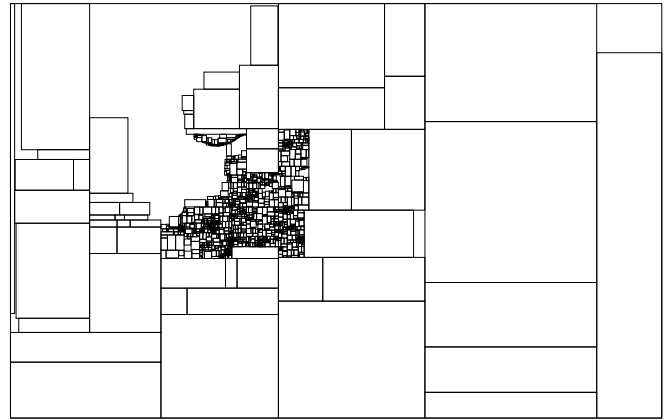
4.2 Dynamic Updates

Bulk loaded indexes can be maintained in the presence of updates using the algorithms of the corresponding dynamic structures. For instance R-trees generated by Hilbert, STR or OMT could utilize the insertion and deletion algorithms of R*-Trees [5], or other variants [6, 16]. However, these algorithms can be expensive (e.g., R*-Trees re-insert all entries of an underflowed node) and unsuitable for update intensive workloads. To alleviate this problem, Waffle [24] determines the update frequency of nodes based on their ratio of queries over updates, using two parameters *fat* and *tolerance*, so that only frequently queried nodes are continuously updated.

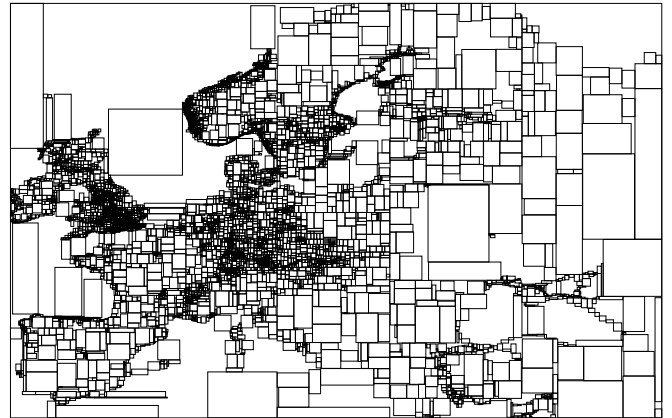
The proposed adaptive techniques provide a natural way to handle workload-based dynamic updates. Specifically, when a new point causes a leaf node to overflow, a new page is allocated to the node to accommodate that point as well as future insertions. Eventually, the node will be processed and refined, when it is accessed by some query. Similarly, underflows are only handled when the node is queried. Unlike Waffle, this lazy approach does not require the maintenance of statistical information per node (the counter of queries and updates), or the introduction of additional parameters (*fat* and *tolerance*). Compared to existing algorithms for dynamic



(a) AMBI after 10 window queries focused on Germany



(b) AMBI after 100 window queries focused on Germany



(c) FMBI leaf nodes

Figure 6: Leaf level of Europe (OSM)

multidimensional indexes, this is expected to drop the cost significantly for update intensive workloads, especially when updates arrive in bursts.

5 PARALLEL BULK LOADING AND DISTRIBUTED QUERY PROCESSING

The scan-based nature of the proposed techniques enables their effective extension to distributed systems and spatial partitioning. We assume a central server that receives the data points and queries. The server distributes the data points to m local servers, each responsible for a region of the data space. In this setting FMBI and AMBI can be bulk loaded in parallel, utilizing the resources (e.g., disk, buffer) of all servers. We first discuss the adaptation of FMBI.

Assuming a main memory buffer of M pages, the central server partitions $\gamma \cdot m$ random pages of the dataset, where $\gamma = \lfloor M/m \rfloor$, to m subspaces, using a SplitTree with $m-1$ splits. The γ pages of each subspace n_i are sent to the corresponding local server l_i . Subsequently, every l_i generates a local $FMBI^i$, indexing n_i . Specifically, the central server distributes the points of the remaining $(P - \gamma \cdot m)$ pages to the local servers. Assume that the available buffer at server l_i is M_i . When l_i receives $\delta \cdot C_B$ pages of points within n_i , where $\delta = \lfloor M_i/C_B \rfloor$, it performs its own Step 1, to partition n_i into C_B subspaces. Steps 2 to 5 form these subspaces into the root entries of $FMBI^i$, as discussed in Section 3.

The cost incurred at the global server is equal to the total number P of pages, since it reads the entire dataset once to compute the partitions and distribute the remaining points. Let P_i be the number of data pages for subspace n_i . Each local server l_i creates $FMBI^i$ levels from top to bottom. Assuming that all subspaces are inactive, at each level, it iterates through all the P_i pages, and generates C_B partitions for the next level. After $L = \log_{C_B}(P_i/M_i)$ levels of partitions, the subspaces are partitioned in the main memory. Thus, the cost for each l_i is: $\sum_{l=0}^L C_B^l \frac{P_i}{C_B^l} = P_i \log_{C_B}(P_i/M_i)$. The parallel running time is determined by the local server with the highest cost [4] [32]. If all servers have identical resources, this would be the l_i with the largest number P_i of data pages.

When the central server receives a query, it directs it only to *qualified* local servers, i.e., those that may contribute results. For window queries, qualified servers are those whose subspace intersects the window. However, for nearest neighbor (k -NN) queries there is no predefined range. To overcome this problem, Spatial-Hadoop [10] processes a k -NN query q in two rounds. Round 1 finds k candidate NNs in the server covering q , and computes the distance $dist$ between q and the k -th candidate. Round 2 searches for additional candidates in the local servers whose subspace intersects the circle centered at q with radius $dist$. AQWA [2] processes the query in a single round, using histograms to identify qualified servers. Either method is compatible with the proposed techniques.

The extension of the above to adaptive indexing is straightforward. When the central server receives the first query, it applies Step 1 to build the partition scheme and determine the subspace of each local server. Then, at Step 2 it distributes to every local server the data points within its subspace. Each local server performs Steps 1 to 4, to build a partial AMBI, without incurring additional I/O^4 . The first query is processed by the central server that has to scan the entire data set anyway. When each new query arrives, it

⁴Operations that incur additional I/O , i.e., refinement of inactive (at Step 3) and dense (at Step 5) subspaces are deferred for later.

is directed to the qualified servers, which use the query to refine qualified nodes at their local index as discussed in Section Section 4.

6 EXPERIMENTAL EVALUATION

We compare the proposed FMBI, and its adaptive version AMBI, against the methods discussed in Section 2. We exclude TGS because they are at least an order of magnitude more expensive at bulk loading and query processing than others (as shown in Table 1, most of their nodes are elongated). Similarly, learned indexes are excluded because of their large training time, and pre-requisite workload requirement. For KDB-Trees we include the more efficient *spread* variant [14], bulk loaded by the algorithm of [24]. To ensure fairness, the indexes were implemented within the same disk-based framework that we developed in Rust⁵. All experiments were conducted on an AMD Ryzen Threadripper 3960X 3.8GHz CPU with 64GiB RAM and 64-bit Ubuntu Linux operating system, with a disk-page size of 4KiB. We use the following real data sets:

- (1) OSM [28]: 1 billion 2D geolocations across the globe.
- (2) NYCYT [27]: 100 million 5D trip records of New York City yellow taxis in the year 2014. The dimensions are the x, y coordinates of the pick up and drop off points, and the time.
- (3) Additional experiments with uniform, gaussian, and skewed data are included in the code repository⁵.

The first experiment focuses on the conventional (i.e., non-adaptive) bulk loading of OSM using an LRU buffer equal to 1% of the dataset. Given the page size of 4KiB, the maximum capacity is $C_L = 341$ for leaf nodes, and $C_B = 204$ for branches, in all indexes (branch entries store bounding boxes and require two points per entry, instead of one for leaves). OSM occupies 2932552 disk pages, i.e., the same as the number of leaf nodes of fully packed indexes in Table 1. The 1% buffer size corresponds to 29325 pages, and the value of α in FMBI is $143 = \lfloor 29325/204 \rfloor$, i.e., Step 1 partitions into 204 subspaces, as shown in Figure 4a, each containing 143 full pages. In order to study the effect of sampling in FMBI, we executed the experiment using 100 different samples (each with size 1% of the dataset). The average bulk loading cost in terms of page I/O , i.e., total number of page reads and writes was 11733245, and the maximum (minimum) was 11757239 (11727645). The difference in term of query processing cost are similarly negligible. The reported results correspond to the average values.

The top-left diagram in Figure 7 illustrates the cost of building the full index. The numbers on top of each method indicate its relative performance compared to FMBI. Top-down approaches are the most expensive because they involve numerous applications of external sorting. Specifically, KDB-Trees are the slowest because of the larger number of leaf nodes (see Table 1), followed by Waffle and OMT. For bottom-up approaches, Hilbert outperforms STR because given the available buffer, it only performs external sorting once for the leaf level nodes. FMBI is naturally even faster as it avoids external sorting altogether. Moreover, as shown in the bottom-left diagram, FMBI has the same size as the indexes that pack leaf nodes fully, demonstrating the effectiveness of the merging process at Step 4.

The second column of diagrams in Figure 7 measures the cost of k -nearest neighbor and window queries, as a function of k and

⁵The code will be open sourced post acceptance.

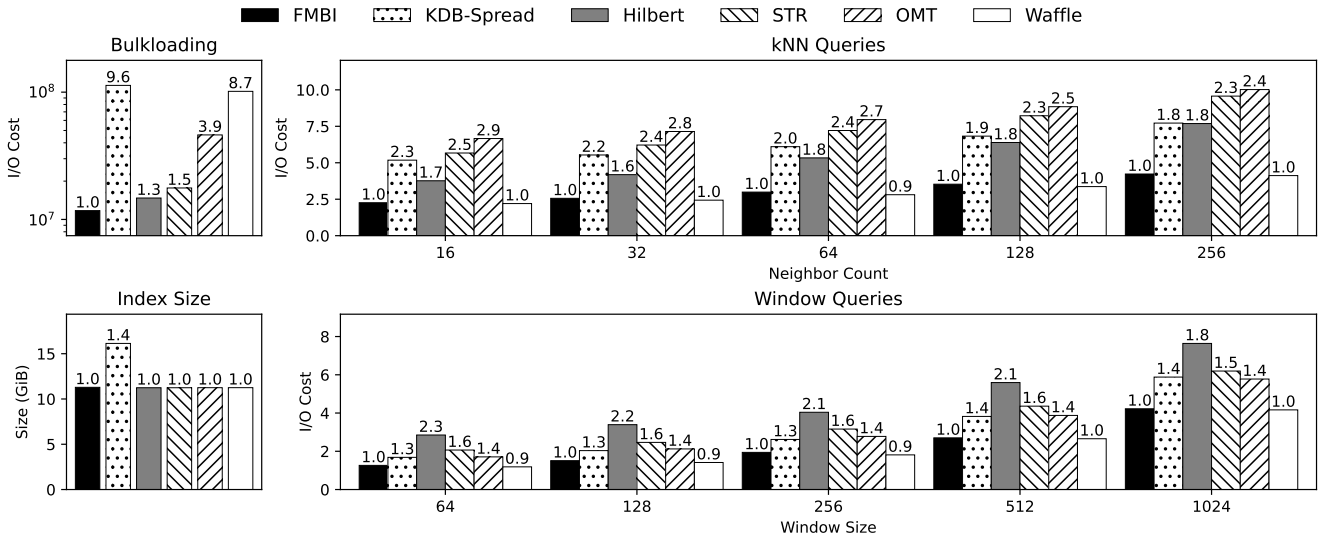


Figure 7: OSM | Non-adaptive

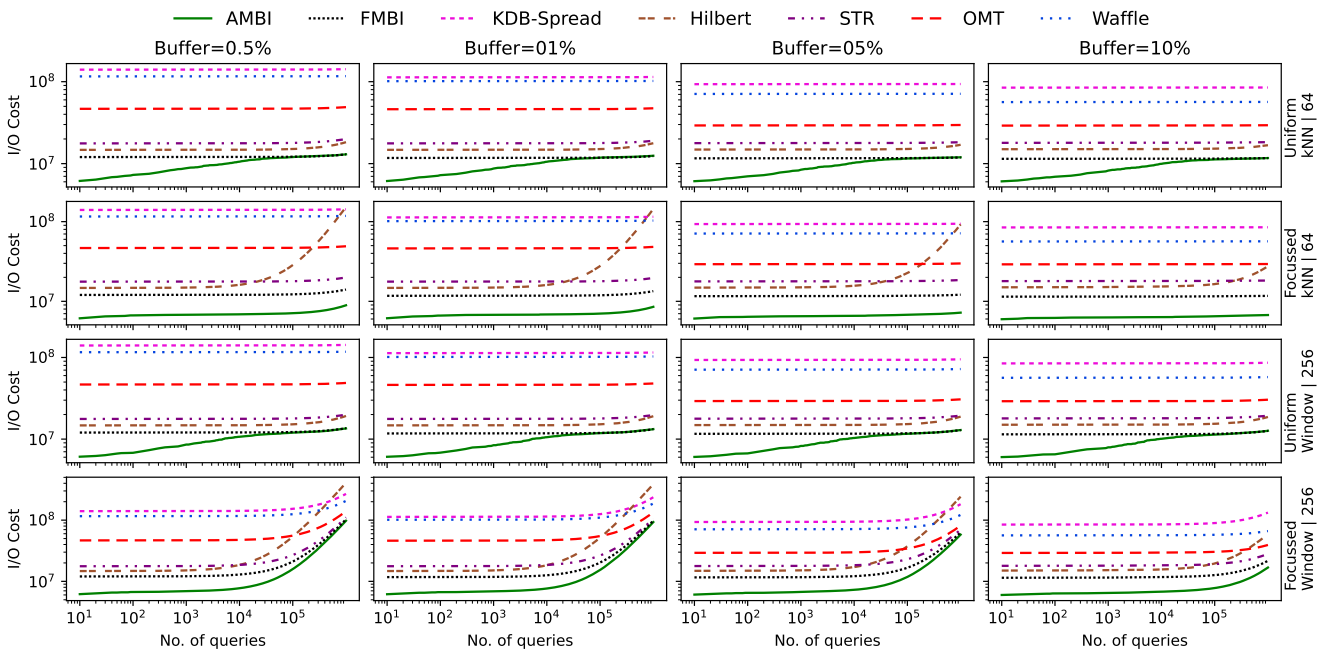


Figure 8: OSM | Adaptive

window size, given the 1% LRU buffer. For k -NN queries, k ranges from 16 to 256. Each window query is a rectangle, whose aspect ratio is the same as the data space, and area is a percentage that ranges between $64/N$ and $1024/N$, where N is the data cardinality. Every reported value is the average of 1000 queries, uniformly spread in the entire data space. As expected, the absolute number of disk pages retrieved increases with the output size for all methods. FMBI is almost as fast as Waffle, which, however, is 8.7 times slower on index building. All other methods are consistently slower for all

settings, which can be explained by the inferior node properties demonstrated in Table 1. The relative performance of these methods depends on the query characteristics.

The next experiment focuses on the adaptive bulk loading of OSM and the performance of AMBI. Each row of plots in Figure 8 corresponds to a query type, and every column to an LRU buffer size that ranges between 0.5% to 10% of the dataset. The diagrams in the first row illustrate the combined I/O cost of index building and 64-NN uniform queries over the entire space. Specifically, for

non-adaptive methods including FMBI, we build the complete index in a single step, perform up to 10^6 64-NN, and plot the total (index building and cumulative query) cost as a function of the number of queries performed. For AMBI, the index is gradually refined as each query is processed. For all buffer sizes, AMBI is the fastest method, usually by orders of magnitude. As expected, the benefits of AMBI are more pronounced for a small number of queries.

According to Figure 7, for non-adaptive methods index building is 6-8 orders of magnitude more expensive than single queries, and, thus, it dominates the total cost. Therefore, there is no visible difference in their performance in Figure 8 as the number of queries reaches 10^6 . FMBI is the most efficient, followed by Hilbert, STR and OMT. Although Waffle has fast query processing, it is the second most expensive overall (after KDB-Trees) due to its high building cost. A large buffer size improves all methods because it leads to lower building cost (the speed of external sorting drops with larger buffer sizes) and better query performance (more index nodes remain in-memory).

The second row of Figure 8 repeats the experiment of the first row, but now all query points are *focused* within the bounding box of Germany, which constitutes a dense area. This has a minimal effect on non-adaptive methods, whose cost is dominated by index building. On the other hand, for AMBI this also affects index building since the partial index only covers space potentially containing query results. Accordingly, AMBI does not converge to FMBI as the number of queries increases, and most of the data space (excluding Germany) remains non indexed (see Figure 6).

Rows 3 and 4 of Figure 8 illustrate the corresponding diagrams for uniform and focused window queries, which are similar to those for k -NN. The main difference is in the last row where the cost of query processing starts becoming visible for FMBI, Hilbert and STR after the first 10^4 queries. This happens because focused window queries in a dense area have large output, and are more expensive than uniform queries of the same size.

Figure 9 evaluates the performance of non-adaptive indexes versus the number d of dimensions using NYCYT. Each row of plots corresponds to a different value of d between 2 and 5. When $d < 5$, we select the first d dimensions of the dataset. As shown in the diagrams of the left column, FMBI is the fastest to build for all values of d , while having the same size as the fully packed indexes⁶. Regarding query processing, all queries are uniformly distributed in the data space. The absolute cost of all methods increases with d , as the tree fan-out decreases due to the additional dimensions. The effect is more evident on k -NN queries due to the dimensionality curse [7], i.e., the volume of space that must be searched for candidate neighbors grows exponentially with d . Similar to the experiments for OSM, FMBI and Waffle are the most efficient for every query setting (but Waffle is 8.2 to 8.6 times slower to build). Compared to Figure 7 the difference of the other methods relative to FMBI is lower because NYCYT is less skewed (e.g., it does not contain empty areas such as the oceans of OSM). However, the relative difference gradually increases with d , indicating that FMBI (and Waffle) scales better with the data dimensionality.

⁶For $d = 5$, the bulk loading procedure of OMT cannot pack nodes to their full capacity, which affects both the index size and the query performance.

Figure 10 focuses on the adaptive bulk loading of NYCYT. In each diagram, we measure the combined index building and cumulative query cost versus the number of queries performed, using an LRU buffer with size equal to 1% of the dataset. Every row of diagrams corresponds to a query type and every column to a dimensionality d value. For both k -NN and window queries, as well as for both uniform and focused⁷ distributions, the total cost increases with d , due to query processing; according to Figure 9, an average query for $d = 5$ is about an order of magnitude more expensive than for $d = 2$. FMBI outperforms all non-adaptive competitors for every setting since it combines fast index building and efficient query processing. Compared to Figure 8, AMBI converges faster to FMBI. Moreover as the dimensionality increases, the difference between uniform and focused queries diminishes due to the dimensionality curse.

The final set of experiments evaluates parallel bulk loading and query processing in distributed systems with a central server and m local servers, as discussed in Section 5. The leftmost diagrams in Figure 11 illustrate the cost of building FMBI versus m , for NYCYT and values of d between 2 and 5. The horizontal red line is the cost of scanning the entire data set at the central server, which is independent of m . Each server has a buffer which is equal to $\frac{5\%}{m}$ of the entire dataset. The number on top of each column indicates the relative performance with respect to a centralized architecture ($m = 1$). For $m > 1$, the cost is determined by the slowest local server [4] [32], i.e., the one with the densest subspace, given that all servers have identical buffers. Naturally, as the number of local servers increases, the maximum cost decreases, indicating that FMBI scales well with the number of servers because, as discussed in the context of Figure 4a FMBI achieves well balanced partitioning. The next set of plots in Figure 11 measures the cost of window query processing as a function of m . Specifically, the reported value is the number of page accesses per query, when processing 1000 uniform window queries in parallel. The parallel running time is again determined by the slowest server. As expected the cost drops as the number of servers increases. Although the actual cost grows with the dimensionality, the relative advantage of multiple local servers remains consistent.

7 CONCLUSION

This paper presents novel scan-based methods for bulk loading disk-based multidimensional points. Our first contribution is FMBI, a full index that clearly outperforms all external sort-based schemes in terms of indexing and query cost. Waffle, the only technique comparable to FMBI on query performance, is 8.2 to 8.7 times slower on index building. The adaptive version AMBI generates a partial index on demand, as a response to queries, and has substantial benefits, especially when queries are focused on a small part of the data space. Both FMBI and AMBI are naturally extended to distributed systems, where index building and query processing take advantage of multiple servers to enhance efficiency.

⁷In focused queries, the query point or window lies within a 10% volume at the center of the dataset.

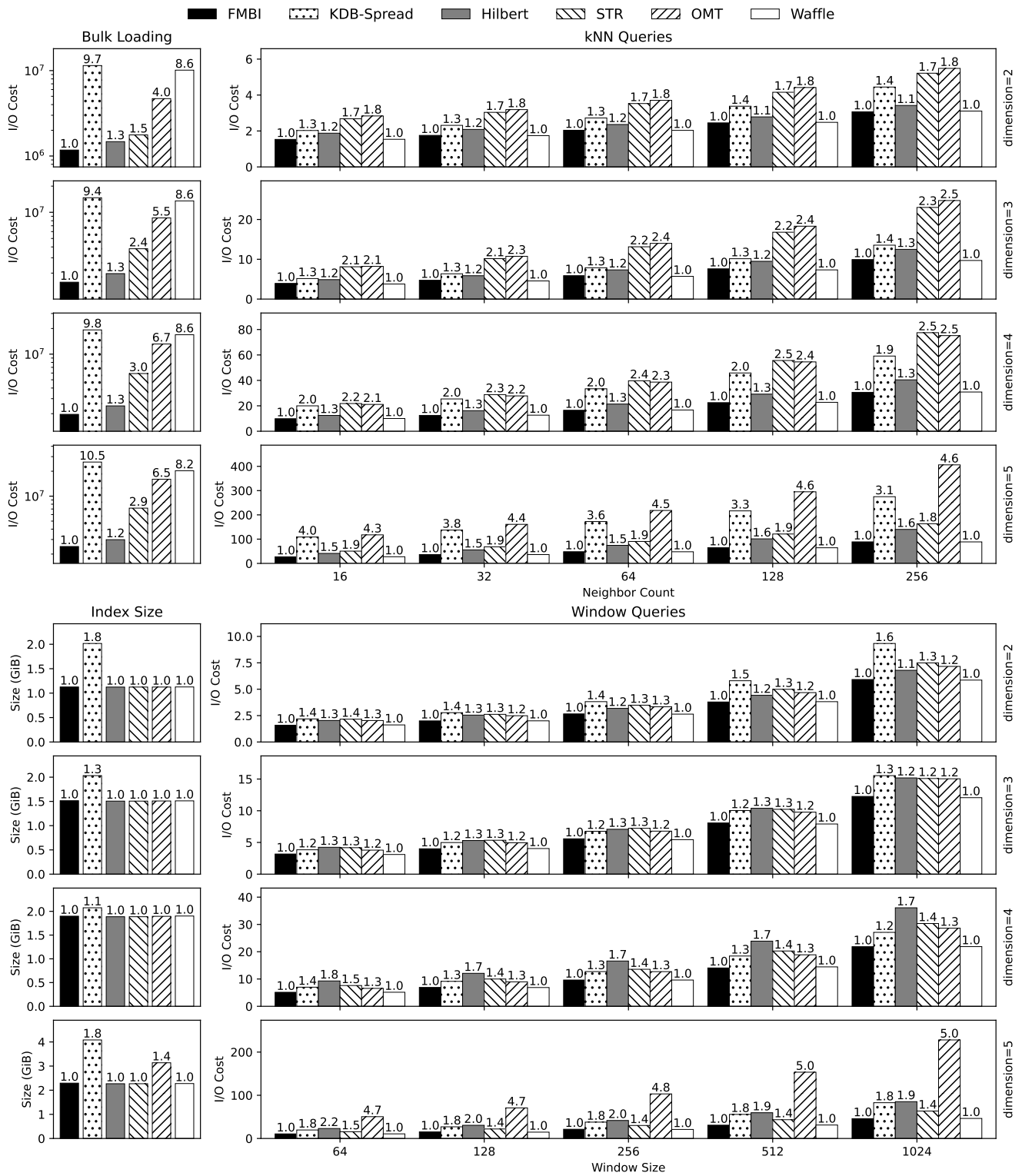


Figure 9: NYCYT | Non-adaptive

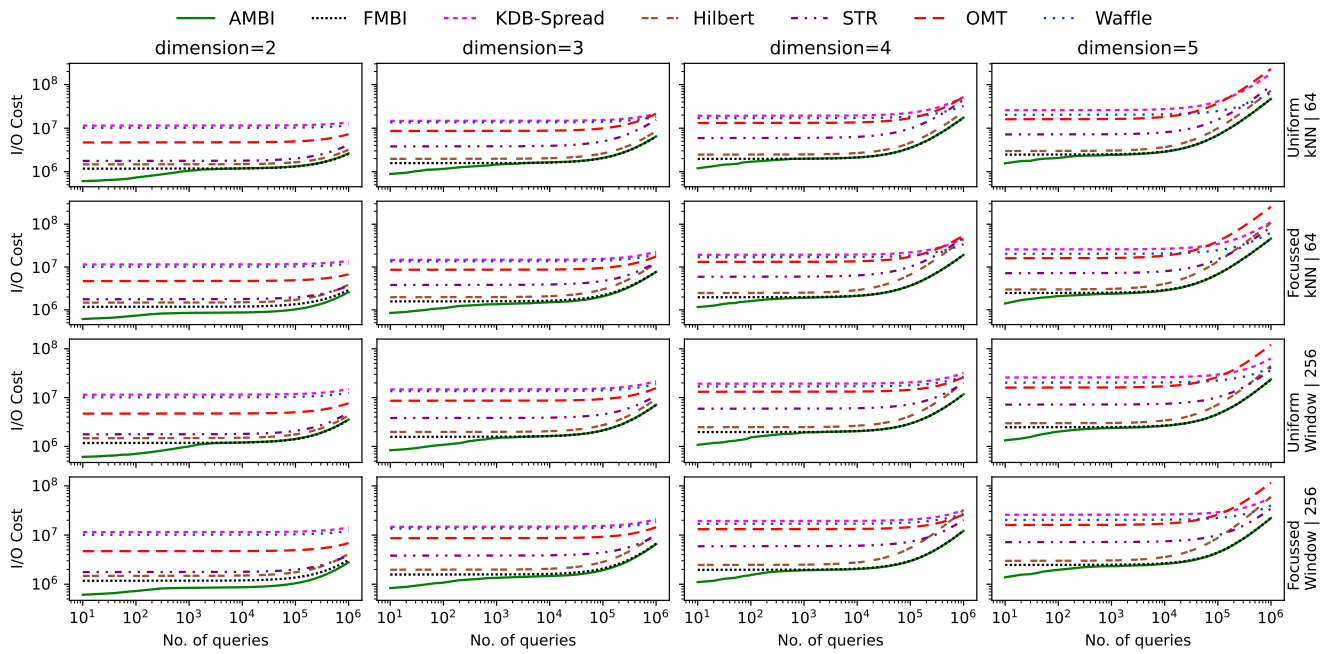


Figure 10: NYCYT | Adaptive

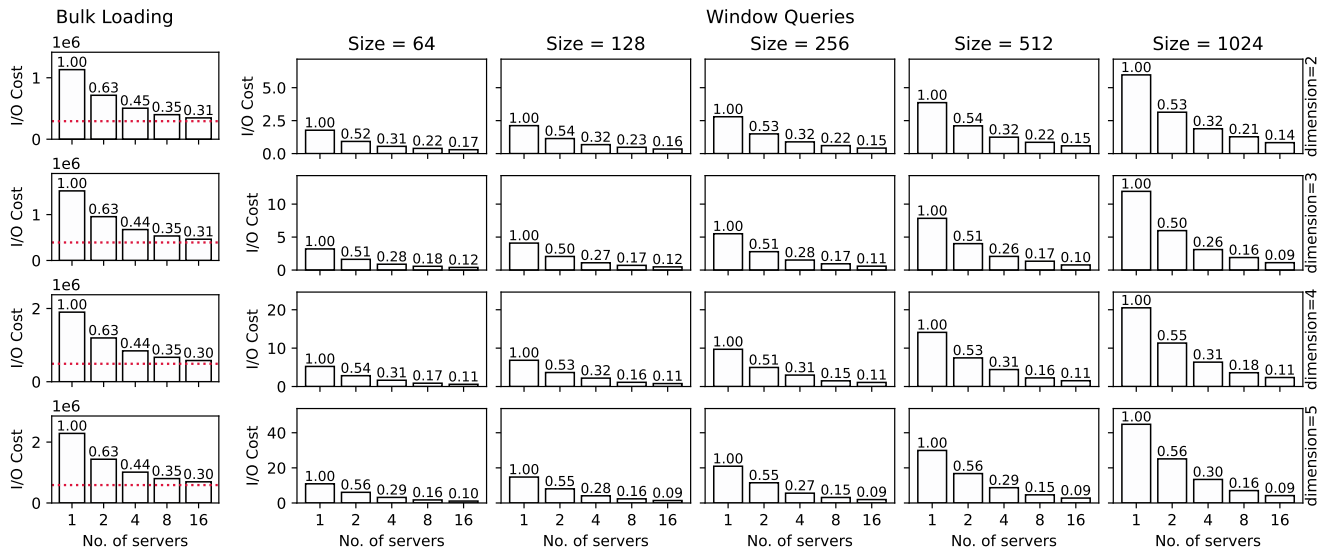


Figure 11: NYCYT | Non-Adaptive | Parallel

REFERENCES

- [1] Daniar Achakeev, Bernhard Seeger, and Peter Widmayer. 2012. Sort-based query-adaptive loading of R-trees. *ACM International Conference Proceeding Series*, 2080–2084. <https://doi.org/10.1145/2396761.2398577>
- [2] Ahmed M. Aly, Ahmed R. Mahmoud, Mohamed S. Hassan, Walid G. Aref, Mourad Ouzzani, Hazem Elmelegy, and Thamer Qadah. 2015. AQWA: adaptive query workload aware partitioning of big spatial data. *Proceedings of the VLDB Endowment* 8, 13 (Sept. 2015), 2062–2073. <https://doi.org/10.14778/2831360.2831361>
- [3] Lars Arge, Mark de Berg, Herman J. Haverkort, and Ke Yi. 2004. The Priority R-tree: a practically efficient and worst-case optimal R-tree. In *Proceedings of the 2004 ACM SIGMOD international conference on Management of data*. ACM, Paris France, 347–358. <https://doi.org/10.1145/1007568.1007608>
- [4] Paul Beame, Paraschos Koutris, and Dan Suciu. 2013. Communication steps for parallel query processing. In *Proceedings of the 32nd ACM SIGMOD-SIGACT-SIGAI symposium on Principles of database systems (SIGMOD/PODS’13)*. ACM. <https://doi.org/10.1145/2463664.2465224>
- [5] Norbert Beckmann, Hans-Peter Kriegel, Ralf Schneider, and Bernhard Seeger. 1990. The R*-tree: an efficient and robust access method for points and rectangles. In *Proceedings of the 1990 ACM SIGMOD international conference on Management of data*. ACM, Atlantic City New Jersey USA, 322–331. <https://doi.org/10.1145/93597.98741>
- [6] Norbert Beckmann and Bernhard Seeger. 2009. A revised r*-tree in comparison with related index structures. In *Proceedings of the 2009 ACM SIGMOD International Conference on Management of data*. ACM, Providence Rhode Island USA, 799–812. <https://doi.org/10.1145/1559845.1559929>
- [7] Kevin Beyer, Jonathan Goldstein, Raghu Ramakrishnan, and Uri Shaft. 1999. When Is “Nearest Neighbor” Meaningful? Springer Berlin Heidelberg, 217–235. https://doi.org/10.1007/3-540-49257-7_15
- [8] Jialin Ding, Vikram Nathan, Mohammad Alizadeh, and Tim Kraska. 2020. Tsunami: a learned multi-dimensional index for correlated data and skewed workloads. *Proceedings of the VLDB Endowment* 14, 2 (Oct. 2020), 74–86. <https://doi.org/10.14778/3425879.3425880>
- [9] Ahmed Eldawy and Mohamed F. Mokbel. 2015. SpatialHadoop: A MapReduce framework for spatial data. In *2015 IEEE 31st International Conference on Data Engineering*. 1352–1363. <https://doi.org/10.1109/ICDE.2015.7113382>
- [10] Ahmed Eldawy and Mohamed F. Mokbel. 2015. SpatialHadoop: A MapReduce framework for spatial data. In *2015 IEEE 31st International Conference on Data Engineering*. IEEE. <https://doi.org/10.1109/icde.2015.7113382>
- [11] Ahmed Eldawy, Mohamed F. Mokbel, Saif Alharthi, Abdulhadi Alzaidy, Kareem Tarek, and Sohaib Ghani. 2015. SHAHED: A MapReduce-based system for querying and visualizing spatio-temporal satellite data. In *2015 IEEE 31st International Conference on Data Engineering*. 1585–1596. <https://doi.org/10.1109/ICDE.2015.7113427>
- [12] Ahmed Eldawy, Ibrahim Sabek, Mostafa Elganainy, Ammar Bakeer, Ahmed Abdelmoteleb, and Mohamed F. Mokbel. 2017. Sphinx: Empowering Impala for Efficient Execution of SQL Queries on Big Spatial Data. In *Advances in Spatial and Temporal Databases*, Michael Gertz, Matthias Renz, Xiaofang Zhou, Erik Hoel, Wei-Shinn Ku, Agnes Voisard, Chengyang Zhang, Haiquan Chen, Liang Tang, Yan Huang, Chang-Tien Lu, and Siva Ravada (Eds.). Springer International Publishing, Cham, 65–83.
- [13] A. J. Fisher. 1986. A new algorithm for generating hilbert curves. *Software: Practice and Experience* 16, 1 (Jan. 1986), 5–12. <https://doi.org/10.1002/spe.4380160103>
- [14] Jerome H. Friedman, Jon Louis Bentley, and Raphael Ari Finkel. 1977. An Algorithm for Finding Best Matches in Logarithmic Expected Time. *ACM Trans. Math. Software* 3, 3 (Sept. 1977), 209–226. <https://doi.org/10.1145/355744.355745>
- [15] Yván J. García R, Mario A. López, and Scott T. Leutenegger. 1998. A greedy algorithm for bulk loading R-trees. In *Proceedings of the 6th ACM international symposium on Advances in geographic information systems*. ACM, Washington D.C. USA, 163–164. <https://doi.org/10.1145/288692.288723>
- [16] Antonin Guttman. 1984. R-trees: a dynamic index structure for spatial searching. In *Proceedings of the 1984 ACM SIGMOD international conference on Management of data - SIGMOD ’84*. ACM Press, Boston, Massachusetts, 47. <https://doi.org/10.1145/602259.602266>
- [17] Stratos Idreos, Martin L. Kersten, and Stefan Manegold. 2007. Database Cracking. In *Proceedings of the 3rd International Conference on Innovative Data Systems Research (CIDR)*. Asilomar, California, 68–78.
- [18] Anders Hammershøj Jensen, Frederik Möllerström Lauridsen, Fatemeh Zardbani, Stratos Idreos, and Panagiotis Karras. 2021. Revisiting Multidimensional Adaptive Indexing [Experiment & Analysis]. In *International Conference on Extending Database Technology*. <https://api.semanticscholar.org/CorpusID:232283671>
- [19] Ibrahim Kamel and Christos Faloutsos. 1993. On packing R-trees. In *Proceedings of the second international conference on Information and knowledge management - CIKM ’93*. ACM Press, Washington, D.C., United States, 490–499. <https://doi.org/10.1145/170088.170403>
- [20] Richard M. Karp, Rajeev Motwani, and Prabhakar Raghavan. 1988. Deferred Data Structuring. *SIAM J. Comput.* 17, 5 (1988), 883–902. <https://doi.org/10.1137/0217055>
- [21] Taewon Lee and Sukho Lee. 2003. OMT: Overlap Minimizing Top-down Bulk Loading Algorithm for R-tree. In *The 15th Conference on Advanced Information Systems Engineering (CAISE ’03), Klagenfurt/Velden, Austria, 16-20 June, 2003, CAISE Forum, Short Paper Proceedings, Information Systems for a Connected Society (CEUR Workshop Proceedings, Vol. 74)*, Johann Eder and Tatjana Welzer (Eds.). CEUR-WS.org.
- [22] S.T. Leutenegger, M.A. Lopez, and J. Edgington. 1997. STR: a simple and efficient algorithm for R-tree packing. In *Proceedings 13th International Conference on Data Engineering*. IEEE Comput. Soc. Press, Birmingham, UK, 497–506. <https://doi.org/10.1109/ICDE.1997.582015>
- [23] Pengfei Li, Hua Lu, Qian Zheng, Long Yang, and Gang Pan. 2020. LISA: A Learned Index Structure for Spatial Data. In *Proceedings of the 2020 ACM SIGMOD International Conference on Management of Data*. ACM, Portland OR USA, 2119–2133. <https://doi.org/10.1145/3318464.3389703>
- [24] Moin Hussain Moti, Panagiotis Simatis, and Dimitris Papadias. 2022. Waffle: A Workload-Aware and Query-Sensitive Framework for Disk-Based Spatial Indexing. *Proceedings of the VLDB Endowment* 16, 4 (Dec. 2022), 670–683. <https://doi.org/10.14778/3574245.3574253>
- [25] Vikram Nathan, Jialin Ding, Mohammad Alizadeh, and Tim Kraska. 2020. Learning Multi-Dimensional Indexes. In *Proceedings of the 2020 ACM SIGMOD International Conference on Management of Data*. ACM, Portland OR USA, 985–1000. <https://doi.org/10.1145/3318464.3380579>
- [26] Matheus Agio Nerone, Pedro Holanda, Eduardo C. de Almeida, and Stefan Manegold. 2021. Multidimensional Adaptive & Progressive Indexes. In *2021 IEEE 37th International Conference on Data Engineering (ICDE)*. 624–635. <https://doi.org/10.1109/ICDE51399.2021.00060>
- [27] NYC OpenData. 2017. 2014 Yellow Taxi Trip Data. <https://data.cityofnewyork.us/Transportation/2014-Yellow-Taxi-Trip-Data/gknc-dk5s>
- [28] OpenStreetMap contributors. 2017. Planet dump retrieved from <https://planet.osm.org>. <https://www.openstreetmap.org>
- [29] Apostolos Papadopoulos and Yannis Manolopoulos. 2003. Parallel bulk-loading of spatial data. *Parallel Comput.* 29 (10 2003), 1419–1444. <https://doi.org/10.1016/j.parco.2003.05.003>
- [30] Mirjana Pavlovic, Darius Sidlauskas, Thomas Heinis, and Anastasia Ailamaki. 2018. QUASII: QUery-Aware Spatial Incremental Index. In *Proceedings of the 21st International Conference on Extending Database Technology, EDBT 2018*. Open-Proceedings.org. <https://doi.org/10.5441/002/EDBT.2018.29>
- [31] Jianzhong Qi, Guanli Liu, Christian S. Jensen, and Lars Kulik. 2020. Effectively learning spatial indices. *Proceedings of the VLDB Endowment* 13, 12 (Aug. 2020), 2341–2354. <https://doi.org/10.14778/3407790.3407829>
- [32] Jianzhong Qi, Yufei Tao, Yanchuan Chang, and Rui Zhang. 2020. Packing R-trees with Space-filling Curves: Theoretical Optimality, Empirical Efficiency, and Bulk-loading Parallelizability. *ACM Transactions on Database Systems* 45, 3 (Sept. 2020), 1–47. <https://doi.org/10.1145/3397506>
- [33] John T. Robinson. 1981. The K-D-B-tree: a search structure for large multidimensional dynamic indexes. In *Proceedings of the 1981 ACM SIGMOD international conference on Management of data - SIGMOD ’81*. ACM Press, Ann Arbor, Michigan, 10. <https://doi.org/10.1145/582318.582321>
- [34] Nick Roussopoulos and Daniel Leifker. 1985. Direct spatial search on pictorial databases using packed R-trees. In *Proceedings of the 1985 ACM SIGMOD international conference on Management of data*. ACM, Austin Texas USA, 17–31. <https://doi.org/10.1145/318898.318900>
- [35] Yufei Tao and Dimitris Papadias. 2002. Adaptive Index Structures. In *Proceedings of 28th International Conference on Very Large Data Bases, VLDB 2002, Hong Kong, August 20-23, 2002*. Morgan Kaufmann, 418–429. <https://doi.org/10.1016/B978-155860869-6/50044-5>
- [36] Hoang Vo, Abhimut Aji, and Fusheng Wang. 2014. SATO: a spatial data partitioning framework for scalable query processing. In *Proceedings of the 22nd ACM SIGSPATIAL International Conference on Advances in Geographic Information Systems (Dallas, Texas) (SIGSPATIAL ’14)*. Association for Computing Machinery, New York, NY, USA, 545–548. <https://doi.org/10.1145/2666310.2666365>
- [37] Tin Vu and Ahmed Eldawy. 2020. R*-Grove: Balanced Spatial Partitioning for Large-Scale Datasets. *Frontiers in Big Data* 3 (2020). <https://doi.org/10.3389/fdata.2020.00028>
- [38] Haixin Wang, Xiaoyi Fu, Jianliang Xu, and Hua Lu. 2019. Learned Index for Spatial Queries. In *2019 20th IEEE International Conference on Mobile Data Management (MDM)*. IEEE, Hong Kong, Hong Kong, 569–574. <https://doi.org/10.1109/MDM.2019.00121>
- [39] Dong Xie, Feifei Li, Bin Yao, Gefei Li, Liang Zhou, and Minyi Guo. 2016. Simba: Efficient In-Memory Spatial Analytics. In *Proceedings of the 2016 International Conference on Management of Data (San Francisco, California, USA) (SIGMOD ’16)*. Association for Computing Machinery, New York, NY, USA, 1071–1085. <https://doi.org/10.1145/2882903.2915237>
- [40] Jingyi Yang and Gao Cong. 2023. PLATON: Top-down R-tree Packing with Learned Partition Policy. *Proceedings of the ACM on Management of Data* 1, 4 (Dec. 2023), 1–26. <https://doi.org/10.1145/3626742>
- [41] Jia Yu, Jinxuan Wu, and Mohamed Sarwat. 2015. GeoSpark: a cluster computing framework for processing large-scale spatial data. In *Proceedings of the 23rd SIGSPATIAL International Conference on Advances in Geographic Information*

Systems (Seattle, Washington) (*SIGSPATIAL '15*). Association for Computing Machinery, New York, NY, USA, Article 70, 4 pages. <https://doi.org/10.1145/2820783.2820860>

[42] Fatemeh Zardbani, Nikos Mamoulis, Stratos Idreos, and Panagiotis Karras. 2023. Adaptive Indexing of Objects with Spatial Extent. *Proceedings of the VLDB Endowment* 16, 9 (May 2023), 2248–2260. <https://doi.org/10.14778/3598581.3598596>